Catal Lett (2012) 142:1244–1250
DOI 10.1007/s10562-012-0881-6

High Electrocatalytic Performance of NH_3-Activated Iron-Adsorbed Polyaniline for Oxygen Reduction Reactions

So Jeong Kim · Kee Suk Nahm · Pil Kim

Received: 13 April 2012 / Accepted: 18 July 2012 / Published online: 4 August 2012

Abstract We demonstrate how a highly active non-precious metal-based catalyst for oxygen reduction reactions (ORRs) can be prepared using commercially available polyaniline (PANI) as both nitrogen source and carbon precursor. To do this, PANI-derived catalysts are prepared by pyrolyzing PANI and Fe-impregnated PANI (Fe-PANI) in either N_2 or NH_3 atmospheres. When the catalyst precursor is pyrolyzed under an NH_3 stream, the resultant catalysts (PANI-A and Fe-PANI-A; A denotes treatment with ammonia) have higher microporosities and pyridinic nitrogen contents than those of N_2-pyrolyzed catalysts (PANI-N and Fe-PANI-N; N denotes treatment with nitrogen). Microporosity produced by pyrolysis and pyridinic nitrogen contents are important factors for ORR activity, which is borne out by the better ORR performance of NH_3-pyrolyzed catalysts compared to N_2-pyrolyzed samples. In addition, Fe species coordinated with nitrogen serve as a highly active site to facilitate ORR, leading to Fe-PANI-A delivering the best ORR performance among the PANI-derived catalysts. The onset and half-wave potentials of Fe-PANI-A for ORR were measured as 0.916 and 0.787 mV, respectively, better than for commercial Pd/C. Although some degradation in ORR activity of Fe-PANI-A is observed after a durability test, the loss in the half-wave potential is only 52 mV, indicating a relatively stable ORR activity for Fe-PANI-A.

S. J. Kim · K. S. Nahm · P. Kim (✉)
Department of Hydrogen and Fuel Cell Engineering, Specialized Graduate School, Chonbuk National University, Jeonju 561-756, South Korea
e-mail: kimpil1@chonbuk.ac.kr

K. S. Nahm · P. Kim
School of Semiconductor and Chemical Engineering, Chonbuk National University, Jeonju 561-756, South Korea

Keywords Oxygen reduction reaction (ORR) · Non-precious metal catalyst · Polyaniline (PANI) · Cathode catalyst · Polymer electrolyte fuel cells (PEMFCs)

1 Introduction

Polymer electrolyte fuel cells (PEMFCs) are electrochemical energy conversion devices that can generate efficient and clean power suitable for driving zero-emission electric vehicles [1–3]. To overcome large overpotentials and thus increase energy conversion efficiency, Pt-based materials are currently employed as the electrocatalysts for both hydrogen oxidation reactions (HORs) at the anode and oxygen reduction reactions (ORRs) at the cathode [4]. However, due to kinetically sluggish ORRs, as compared to HOR, a relatively large amount of Pt would need to be used at the cathode, making PEMFCs too expensive to be applied as practical power sources. For the widespread application of PEMFCs, therefore, a low-cost ORR catalyst with high performance must be developed.

Pd-based alloys have been reported to have high ORR performance even comparable to those of Pt-based materials [5–7]. Although Pd can be currently supplied with a lower cost than Pt, it is also a precious metal element and one should note its scarcity as well as limited availability. In this regard, considerable effort has been focused on the design of non-precious metal-based ORR electrocatalysts [8–25]. Among the catalysts reported so far, nitrogen-containing carbon-Fe or Co composites (M/N/C; M is either Fe or Co) are widely recognized as the most promising alternatives to precious metal-based catalysts [8–22]. M/N/C catalysts are usually prepared by pyrolyzing M-adsorbed carbon at a high temperature. One critical factor determining the ORR activity of this class of

material is found to be the nitrogen content in a specific electronic state; that is, the higher content of pyridinic nitrogen an M/N/C electrocatalyst contains, the better ORR performance it facilitates [8, 14–18]. Therefore, the ORR performance of M/N/C catalysts would be closely related to the nitrogen source as well as the activation conditions employed during the catalyst preparation.

A variety of nitrogen sources including NH_3 [8, 9, 13, 16], chelating agents with nitrogen donors [8, 22], and nitrogen-containing polymers [11, 17] have been employed to create active sites during heat treatment. When NH_3 has been used as a nitrogen source, the catalytic activity has been reported to be evolved by pyrolyzing Fe-adsorbed carbon under a pure NH_3 stream [8, 9, 14, 16]. Due to the etching effect of NH_3, the pyrolyzed material obtained has shown a large portion of micropores, in which Fe-coordinated nitrogen compounds such as FeN_2 and FeN_4 hosted and served as active sites for ORR [8, 13]. On the other hand, recent research has proven that nitrogen-containing polymers such as polyacrylonitrile [17], polypyrrole [11], and polyaniline (PANI) [21] could also be used as a catalyst precursor for M/N/C catalysts with high ORR performance. In particular, a remarkable enhancement in activity and stability was reported by the Zelenay group [21]. They prepared Fe/N/C catalysts using Fe-containing polyaniline-coated carbon followed by a two-step heat treatment in a N_2 atmosphere. The catalytic performance difference between a commercial Pt/C and resultant Fe/N/C was only 43 mV in the half-wave potential.

Although PANI was proven to be a favorable precursor for high ORR performance, it is important to note that a further enhancement in the catalytic activity can be achieved using the same nitrogen source under a different preparation condition, and thus provide valuable information for the design of non-precious metal catalysts with high ORR performance. In this study, we prepared non-precious metal-based ORR catalysts using PANI as both a nitrogen source and carbon precursor. To investigate the effect of additional nitrogen sources and non-precious metal components on the catalytic activity, the catalysts were prepared by pyrolyzing an iron-impregnated PANI and a pure PANI in either NH_3 or N_2 atmospheres. The ORR performance observed was correlated with the properties of the catalysts, which were characterized by XRD, TEM, TEM-EDX, elemental analysis, XPS, N_2-physisorption, and electrochemical measurements.

2 Experimental

2.1 Preparation of PANI-Derived Catalysts

PANI-derived ORR catalysts were prepared by impregnating iron into a commercial PANI sample (Emeraldine base, average molecular weight ~50,000; Sigma-Aldrich), followed by heat treatment. Briefly, the PANI (1 g) was dispersed in an ethanol solution (150 ml) containing $FeCl_3$ (0.03 g; Sigma-Aldrich). After vigorous stirring for 2 h, the solvent was completely evaporated using a rotary evaporator. The powder thus obtained was pyrolyzed at 850 °C for 1 h in either NH_3 or N_2 atmospheres to produce Fe-PANI-A (A refers to the heat treatment in ammonia atmosphere) or Fe-PANI-N (N refers to the heat treatment in nitrogen atmosphere). Two other catalysts, PANI-A and PANI-N, were prepared by the same pyrolysis procedures as those used for Fe-PANI-A and Fe-PANI-N, respectively, but without being impregnated with Fe.

2.2 Characterizations

The morphology of the catalysts was confirmed using TEM (JEOL-2010). The crystalline phases of the catalysts were identified by XRD (Rigaku D/MAX 2500) measurements using CuKα radiation ($\lambda = 1.54056$ Å) operated at 40 kV and 30 mA. The surface electronic states of nitrogen were examined with XPS (AXIS-NOVA (Kratos)). The contents of nitrogen in the catalysts were measured using Element Analyzer (VariO EL). The Fe contents were measured with an electron probe micro analyzer [EPMA, Shimadzu (EPMA-1600)]. Surface area and pore volume were determined by the N_2-physisorption method (ASAP 2010, Micromeritics). The presence of Fe species was confirmed by TEM-EDX (JEM-ARM200F).

Cyclic voltammetry (CV) and linear sweep voltammetry (LSV) were conducted in a conventional three-electrode cell. Pt gauze and Ag/AgCl (Cl-saturated) were used as counter and reference electrodes, respectively. A working electrode was prepared by coating catalyst ink onto the glassy carbon disk of a rotating ring disk electrode (RRDE, PINE(AFE7R9GCPT), disk diameter: 5.61 mm, Pt ring). The ink of PANI-derived catalysts was prepared by a method reported in the literature [22]. For the evaluation of the ORR performance, the LSV was carried out in the potential range—0.215–0.8 V (vs. Ag/AgCl) at a scan rate of 10 mV/s in O_2-saturated $HClO_4$ solution (0.1 M). For the sake of comparison, LSVs over Pd/C (20 wt% Pd on Vulcan carbon; Premetek) was also conducted. The CV was measured from −0.2 to 1.0 V (vs. Ag/AgCl) at a scan rate of 50 mV/s in N_2-purged $HClO_4$ solution (0.1 M). The 20th cycles were taken and are presented in Fig. 4. Hereafter, all the potentials are reported with respect to the reversible hydrogen electrode. The durability test was carried out on two representative catalysts under the same condition as that used for CV experiment except the potential range (0.6–1.0 V) and the number of cycles (1,000 cycles).

3 Results and Discussion

3.1 Physical and Chemical Properties of PANI-Derived Catalysts

Figure 1 shows the XRD patterns of PANI-derived catalysts. No distinct peak is observed for PANI-N and PANI-A, indicative of the amorphous nature of these catalysts [12], while the two Fe-containing catalysts (Fe-PANI-N and Fe-PANI-A) reveal peaks at around 26°, corresponding to the (002) plane of graphite [26], in addition to the characteristic peaks of Fe nitride at 43.5 and 44.5° [27]. The broad (002) peaks for these catalysts imply the graphite phase is deficient in long-range order [12]. The partially graphitized character of Fe-PANI-N and Fe-PANI-A results from the favorable catalytic effect of Fe species on the formation of graphite when a carbon precursor such as PANI is carbonized at high temperature [22]. The Fe contents on both of Fe-PANI-N and Fe-PANI-A were similar to each other (Table 2).

The surface area and pore volume of the catalysts were summarized in Table 1. Compared to the catalysts prepared by N_2-heat treatment (PANI-N and Fe-PANI-N), the NH_3 heat-treated samples (PANI-A and Fe-PANI-A) exhibit higher surface areas and pore volumes. This phenomenon originates from the large number of pores generated by the reaction of NH_3 with carbon, which produces volatile compounds [16]. When Fe is impregnated into PANI, the etching effect of NH_3 would be largely mitigated, as demonstrated by the lower surface area and pore volume of Fe-PANI-A compared to PANI-A. It should be noted that NH_3-pyrolyzed catalysts are highly microporous (87.5 and 84.7 % micropore surface area for PANI-A and Fe-PANI-A, respectively) and expected to be highly active because the active site for ORR would be hosted on the walls of the micropores [12–14, 17]. In contrast, Fe species are likely to be positive for the formation of pores in the absence of

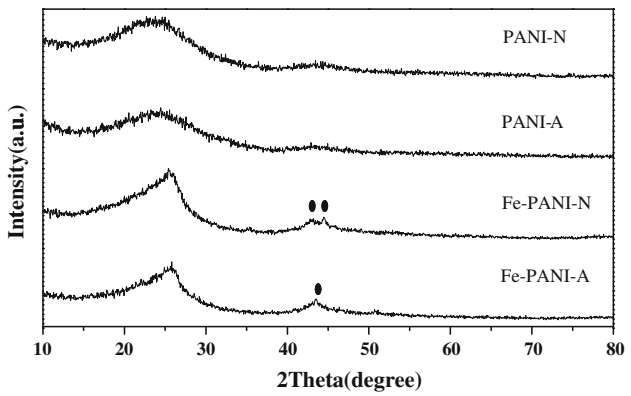

Fig. 1 XRD patterns of PANI-derived catalysts. *Symbol* represents Fe nitride

Table 1 Summary of physical properties of PANI-derived catalysts

Sample	BET surface area (m^2/g)	Micropore area (m^2/g)	Pore volume (cm^3/g)	Micropore volume (cm^3/g)
PANI-N	14.3	4.5	0.05	0.001
PANI-A	1163.7	1018.5	0.55	0.48
Fe-PANI-N	148.9	74.2	0.20	0.03
Fe-PANI-A	649.1	550.0	0.30	0.27

NH_3, as supported by the higher surface area and pore volume of Fe-PANI-N than of PANI-N.

The porous characteristics of PANI-derived catalysts were confirmed by TEM analysis. As shown in Fig. 2, two N_2-pyrolyzed catalysts (PANI-N and Fe-PANI-N) are essentially non-porous while high porosity could be found with NH_3-pyrolyzed samples (PANI-A and Fe-PANI-A). In addition, highly dispersed Fe species for both Fe-PANI-N and Fe-PANI-A are observed in TEM-EDX (Fig. 2e, f, respectively).

The nitrogen contents were measured by elemental analysis, as listed in Table 2. The concentration of nitrogen included in PANI drastically decreased upon pyrolysis. The extent of decrease in nitrogen content is found to vary depending on the pyrolysis conditions and whether or not the Fe was present in the PANI. When Fe is absent in PANI, the NH_3-pyrolysis leads to further decrease in nitrogen content compared to N_2-pyrolysis, indicating that the loss of nitrogen would be accelerated by the presence of NH_3. For Fe-impregnated samples, however, the opposite result is obtained, as Fe-PANI-A shows higher nitrogen content than Fe-PANI-N. This is a result of the effect of Fe on the etching of NH_3, which is inhibited, and the gasification of PANI, which is facilitated [16].

The electronic states of surface nitrogen in the samples were analyzed by XPS. Figure 3 shows the N 1s XPS spectra, including curve fitting for the various nitrogen species present in PANI-derived catalysts. All the spectra were deconvoluted into three sets of binding energies [17], corresponding to pyridinic (398.1 ± 0.1 eV), quaternary (400.7 ± 0.1 eV), and oxidized pyridinic nitrogen (402.8–403.5 eV). As summarized in Table 2, the relative intensities of these nitrogen species depend on the catalyst preparation conditions. For N_2-pyrolyzed catalysts, the pyridinic nitrogen is fitted to be a minor contribution, compared to the quaternary and oxidized pyridinic nitrogens, while it is more developed for NH_3-treated catalysts. Combined with high micro-porosity for PANI-A and Fe-PANI-A, this result demonstrates that NH_3-pyrolysis would be fairly effective for the generation of pyridinic nitrogen on the walls of micropores. Considering that the pyridinic nitrogen hosted in micropores is highly active for

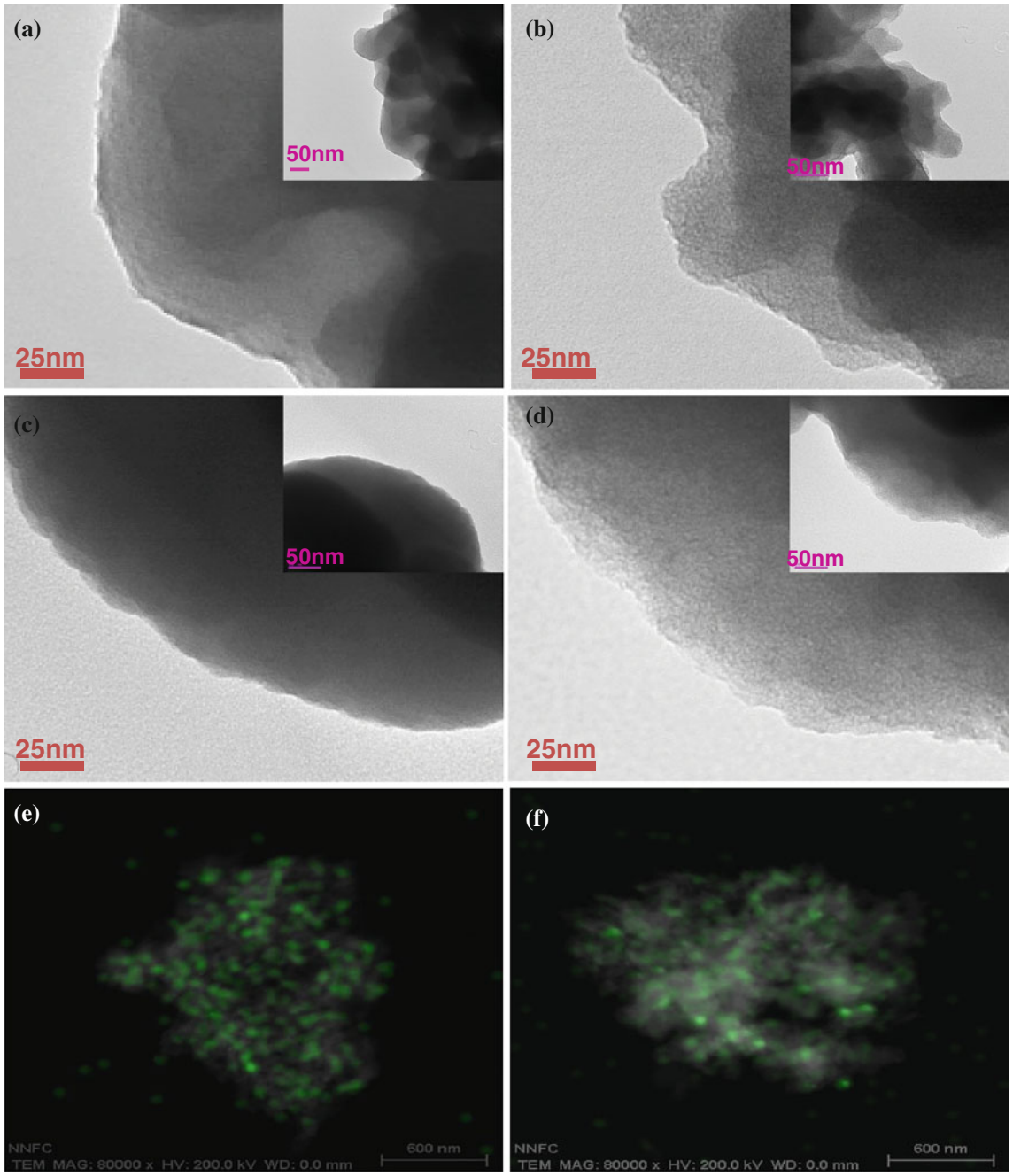

Fig. 2 TEM images of **a** PANI-N, **b** PANI-A, **c** Fe-PANI-N, **d** Fe-PANI-A. **e**, **f** shows TEM-EDX of Fe-PANI-N and Fe-PANI-A, respectively

ORR, NH_3-treated catalysts would be expected to show better performance than N_2-pyrolyzed catalysts.

3.2 Electrochemical Characterization and ORR Performance

Figure 4 shows the cyclic voltammograms for the prepared catalysts in N_2-purged 0.1 M $HClO_4$ solution. The capacitance is observed to increase in the following order: PANI-N < Fe-PANI-N < Fe-PANI-A < PANI-A. This shows a general increase in capacitance for NH_3-treated catalysts over N_2-pyrolyzed ones. This trend in capacitance is similar to that in surface area, which is expected, as the capacitance is closely related to the surface area. The higher surface area the sample has, the larger capacitance it exhibits [28]. The cyclic voltammograms for both PANI-N and PANI-A are featureless, while those for both Fe-PANI-N and Fe-PANI-A reveal a pair of peaks, resulting from Fe^{3+}/Fe^{2+} redox behavior [21].

Table 2 Nitrogen contents, iron contents and the fitting results for the N 1s photoelectron lines

Samples	Nitrogen contents (wt%)[a]	Iron contents (wt%)[b]	XPS (N 1s)		
			Species	Binding energy (eV)	Relative intensity (%)
PANI	17.76	–	–	–	–
PANI-N	7.49	–	Pyridinic N	398.0	18.3
			Quaternary N	400.8	77.8
			Pyridinic N^+O^-	402.8	3.9
Fe-PANI-N	4.47	1.03	Pyridinic N	398.2	20.7
			Quaternary N	400.9	77.0
			Pyridinic N^+O^-	403.5	2.3
PANI-A	6.22	–	Pyridinic N	398.1	34.9
			Quaternary N	400.6	43.7
			Pyridinic N^+O^-	402.8	21.4
Fe-PANI-A	5.34	1.00	Pyridinic N	398.2	34.5
			Quaternary N	400.8	37.0
			Pyridinic N^+O^-	402.9	28.5

[a] Measured by elemental analysis

[b] Measured by electron probe micro analyzer

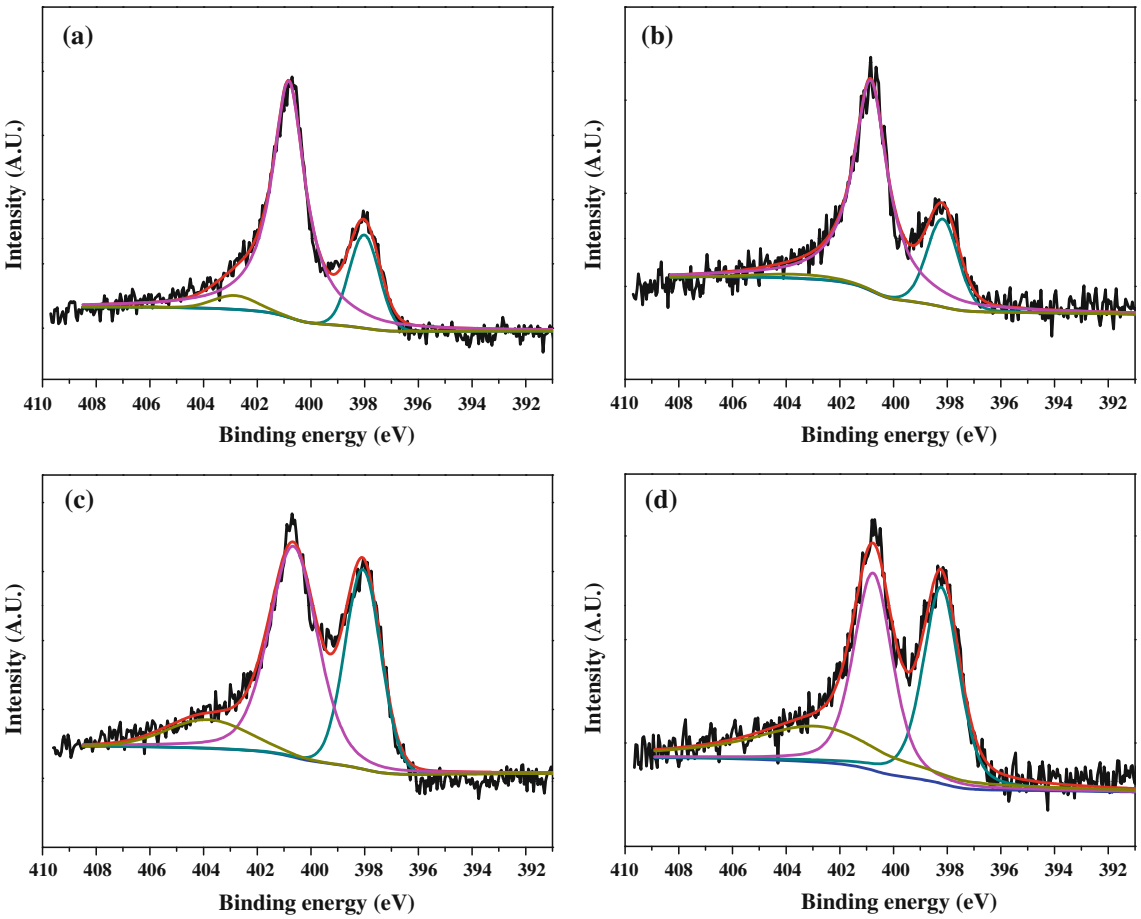

Fig. 3 Deconvoluted N 1s X-ray photoelectron spectra for **a** PANI-N, **b** PANI-A, **c** Fe-PANI-N, and **d** Fe-PANI-A

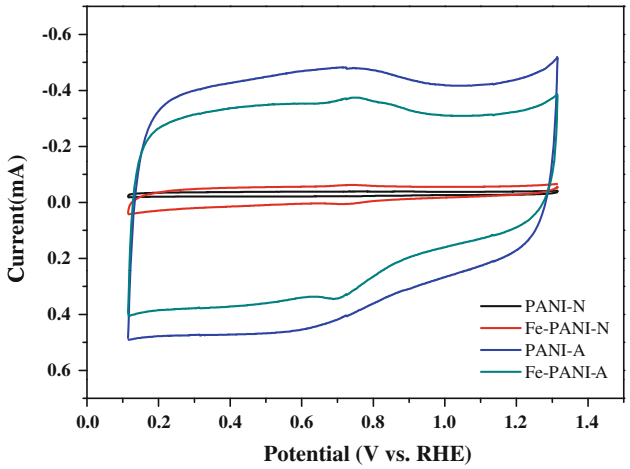

Fig. 4 Cyclic voltammograms obtained with the prepared PANI-derived catalysts in N_2-purged 0.1 M $HClO_4$ solution

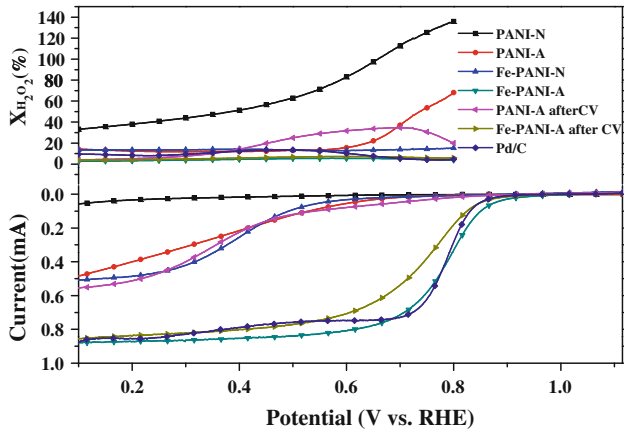

Fig. 5 Disk currents (*lower part*) and the peroxide formation fraction (*upper part*) during ORR. The scan rate and catalyst loading are 10 mV/s and 0.292 mg/cm^2 (16 μg/cm^2 for Pd/C), respectively; Rotating speed of 1,600 rpm; catalyst loadings fixed ring potential at 1.2 V

Figure 5 shows LSV results for the prepared catalysts, which were obtained using a rotating ring disk electrode (RRDE) in an O_2-saturated 0.1 M $HClO_4$ solution. The PANI-N exhibits the lowest onset potential, indicative of the least ORR performance among the PANI-derived catalysts. Although the onset potential of Fe-PANI-N was much larger than PANI-N, the small and ill-defined limiting current of Fe-PANI-N implies a poor ORR performance. A further enhancement in catalytic performance was achieved by pyrolyzing PANI and Fe-PANI in NH_3 atmosphere, shown in PANI-A and Fe-PANI-A. They show well-defined limiting currents and higher half-wave potentials than those of PANI-N and Fe-PANI-N. The most enhanced performance is observed in Fe-PANI-A. The onset and half-wave potentials are 0.916 and 0.787 V, respectively, indicating higher catalytic performance than Pd/C (0.90 and 0.783 V for onset and half-wave potentials, respectively). Although the half-wave potential of Fe-PANI-A is slightly reduced after 1,000 CV cycles, it is within 50 mV of that of Pd/C, implying a relatively stable ORR performance for Fe-PANI-A.

One way to evaluate the catalytic performance of non-precious metal catalysts is to monitor the amount of peroxide formed during ORRs [21, 29–31]. The peroxide formation fraction was calculated by the equation: $\%H_2O_2 = 200 \times I_R/(NI_D + I_R)$, where I_R, I_D, and N represent the ring current, disk current, and collection efficiency (0.37), respectively [32]. As shown in the upper part of Fig. 5, the peroxide formation fraction decreases in the following order: PANI-N > Fe-PANI-N > PANI-A > Fe-PANI-A. In particular, the yield of H_2O_2 with Fe-PANI-A is as low as 3 % in the 0.1–0.8 V potential range, indicating that ORR on Fe-PANI-A was performed mostly by a four-electron transfer [21]. This further confirms the high ORR performance of Fe-PANI-A.

For nitrogen-containing non-precious metal catalysts, the pyridinic [8–19] and, in some case, quaternary nitrogen [17] hosted in micropores are reported to catalyze ORR. In this work, NH_3-treated catalysts have revealed higher microporosities as well as higher pyridinic nitrogen content than N_2-pyrolyzed catalysts. Therefore, it is reasonable to expect superior ORR performances of PANI-A and Fe-PANI-A than either PANI-N and Fe-PANI-N. For NH_3-treated catalysts, Fe-PANI-A showed better ORR performance than PANI-A, though the former had both lower microporosity and overall nitrogen content than the latter catalyst (the proportion of pyridinic and quaternary nitrogen of the total nitrogen contents was nearly the same for both catalysts). It is obvious that the Fe component plays a positive role in enhancing ORR performance. There have been many attempts to elucidate the role of Fe in Fe/N/C catalysts in ORR. One view for the role of Fe is that Fe species serves as active sites for ORR through their coordination with nitrogen in compounds such as in FeN_2 and FeN_4 [8, 9, 13, 14, 16]. On the other hand, the Fe component is also regarded by some not as an active site but as a catalyst for the generation of active sites for ORR [33–35]. Consequently, Fe components would be thought to facilitate the incorporation of pyridinic nitrogen into the carbon matrix. In our case, however, elemental analysis and XPS results showed that the differences in both total nitrogen contents and the relative amount of pyridinic nitrogen between PANI-N and Fe-PANI-A would not be large enough to manifest a difference in ORR performance. Therefore, it is our conclusion that Fe species coordinated with nitrogen in Fe-PANI-A can more easily facilitate ORR than the active site on PANI-A, resulting in large differences in ORR performance.

4 Conclusions

Non-precious metal-based catalysts for ORR were prepared by pyrolyzing PANI and Fe-impregnated PANI at 850 °C in either N_2 or NH_3 atmospheres. PANI-derived catalysts revealed various physical and chemical properties depending on the preparation conditions employed, which affected their ORR performance. It was demonstrated that NH_3-pyrolysis was more favorable for the formation of high microporosity and the incorporation of active pyridinic nitrogen into the produced micropores than N_2-pyrolysis, as is shown by the PANI-A and Fe-PANI-A samples. Consequently, these two catalysts showed higher ORR performances than PANI-N and Fe-PANI-N. Although the micropore surface area of Fe-PANI-A was lower than that of PANI-A, and the difference in pyridinic nitrogen contents between these two catalysts negligible, the former catalyst shows largely improved ORR performance with respect to the latter one. The Fe species coordinating with nitrogen were believed to be highly active for ORR, which was responsible for the highest ORR performance of Fe-PANI-A among the non-precious metal catalysts examined in this study. The catalytic performance of Fe-PANI-A was higher than that of a commercial Pd/C.

Acknowledgments This study was supported by the New & Renewable Energy R&D program (2009T100100606) and the Human Resources Development of the Korea Institute of Energy Technology Evaluation and Planning (KETEP) Grant (20114030200060) funded by the Korean government Ministry of Knowledge Economy. We thank the Jeonju branch of KBSI for XPS measurements and Mr. J. G. Kang at the Center for University Research Facility for his assistance in the measurement of TEM images.

References

1. Steele BCH, Heinzel A (2001) Nature 414:345
2. Larminie J, Dicks A (2003) Fuel cell system explained. John Wiley & Sons, UK
3. Contestabile M, Offer GJ, Slade R, Jaegerc F, Thoennes M (2011) Energy Environ Sci 4:3754
4. Gasteiger HA, Kocha SS, Sompalli B, Wagner FT (2005) Appl Catal B 56:9
5. Fernandez JL, Raghuveer V, Manthiram A, Bard AJ (2005) J Am Chem Soc 127:13100
6. Fernandez JL, Walsh DA, Bard AJ (2005) J Am Chem Soc 127:357
7. Shao MH, Huang T, Liu P, Zhang J, Sasaki K, Vukmirovic MB, Adzic RR (2006) Langmuir 22:10409
8. Lefvre M, Dodelet JP, Bertrand P (2002) J Phys Chem B 106: 8705
9. Jaouen F, Marcotte S, Dodelet JP, Lindbergh G (2003) J Phys Chem B 107:1376
10. Matter PH, Ozkan US (2006) Catal Lett 109:115
11. Bashyam R, Zelenay P (2006) Nature 443:63
12. Matter PH, Zhang L, Ozkan US (2006) J Catal 239:83
13. Herranz J, Lefevre M, Larouche N, Stansfield B, Dodelet JP (2007) J Phys Chem C 111:19033
14. Charreteur F, Jaouen F, Ruggeri S, Dodelet JP (2008) Electrochim Acta 53:2925
15. Shao Y, Sui J, Yin G, Gao Y (2008) Appl Catal B 79:89
16. Lefevre M, Dodelet JP (2008) Electrochim Acta 53:8269
17. Liu G, Li X, Ganesan P, Popov BN (2009) Appl Catal B 93:156
18. Lefevre M, Proietti E, Jaouen F, Dodelet JP (2009) Science 324:71
19. Woods MP, Biddinger EJ, Matter PH, Mirkelamoglu B, Ozkan US (2010) Catal Lett 316:1
20. Ando T, Izhar S, Tominaga H, Nagai M (2010) Electrochim Acta 55:2614
21. Wu G, More KL, Johnston CM, Zelenay P (2011) Science 332:443
22. Heo KC, Nahm KS, Lee SH, Kim P (2011) J Ind Eng Chem 17:304
23. Ishihara A, Lee K, Doi S, Mitsushima S, Kamiya N, Hara M, Domen K, Fukuda K, Ota KI (2005) Electrochem Solid-State Lett 8:A201
24. Zhong HX, Zhang HM, Liu G, Liang YM, Hu JW, Yi BL(2006) Electrochem Commun. 8:707
25. Kim JH, Ishihara A, Mitsushima S, Kamiya N, Ota KI (2007) Electrochim Acta 52:666
26. Joo JB, Kim ND, Yun HJ, Kim P, Yi J (2011) Nano Res 4:92
27. JCPDS-ICDD (2000) Powder Diffract File, #86-0232 (Fe3 N), #73-2102 (Fe2 N)
28. Bard AJ, Faulkner LR (2001) Electrochemical Methods: Fundamentals and applications. John Wiley & Sons, US
29. Beak S, Jung D, Nahm KS, Kim P (2010) Catal Lett 134:288
30. Jung D, Beak S, Nahm KS, Kim P (2010) Korean J Chem Eng 27:1689
31. Jung D, Bae SJ, Kim SJ, Nahm KS, Kim P (2011) Int J Hydrog Energy 36:9115
32. Vukmirovic MB, Zhang J, Sasaki K, Nilekar AU, Uribe F, Mavrikakis M, Adzic RR (2007) Electrochim Acta 52:2257
33. Maldonado S, J.Stevenson K (2004) J Phys Chem B 108:11375
34. Matter PH, Wang E, Ozkan US (2006) J Catal 243:395
35. Nallathambi V, Lee JW, Kumaraguru SP, Wu G, Popov BN (2008) J Power Sources 183:34